



pubs.acs.org/estair Article

# Influence of Application Method on Disinfectant Byproduct Formation during Indoor Bleach Cleaning: A Case Study on Phenol Chlorination

Leif G. Jahn,\* Nirvan Bhattacharyya, Daniel Blomdahl, Mengjia Tang, Pearl Abue, Atila Novoselac, Lea Hildebrandt Ruiz, and Pawel K. Misztal



Cite This: ACS EST Air 2024, 1, 16-24



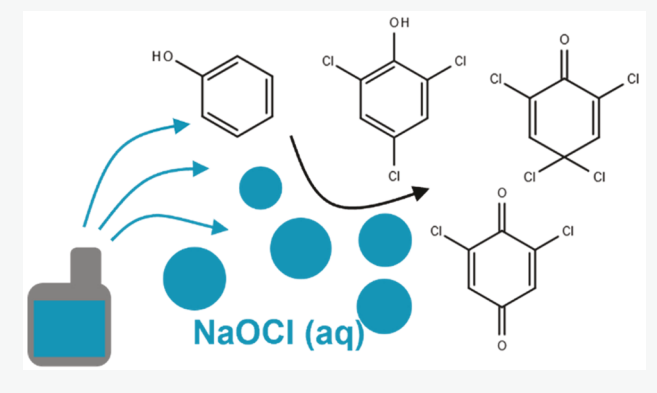
**ACCESS** I

III Metrics & More

Article Recommendations

s Supporting Information

ABSTRACT: Modern disinfection methods increasingly utilize droplet dispersal as a means of delivering disinfectant within an indoor space. Such an application produces droplets over wide size ranges, some of which may remain airborne for minutes to hours while serving as small reaction environments. We report here the formation of chlorophenolic disinfection byproducts (DBPs) during the injection of bleach microdroplets into an environmental chamber. These reactions within airborne microdroplets are driven by phenol dissolution and availability, and the observed DBPs span multiple generations of chlorination chemistry. DBPs representing successive chlorine addition to the phenol ring are initially observed (mono-, di-, and trichlorophenol), followed by DBPs that lack aromaticity (2,6-dichlorobenzoquinone and 2,4,4,6-tetrachloro-2,5-



cyclohexadienone, among others). Chlorophenolic DBPs have not been reported during prior work examining indoor bleach cleaning and we attribute their observation in this work to the dispersal of disinfectant microdroplets rather than traditional mopping or wiping with a bulk aqueous solution on an indoor surface. Airborne microdroplets represent unique reaction and volatilization environments and unique exposure pathways to DBPs, via direct compound inhalation as well as the inhalation of DBP-containing microdroplets. The observed DBPs (particularly 2,6-dichlorobenzoquinone) have previously been linked to adverse health effects in humans through either direct toxicity or as precursors to other DBPs with adverse health effects. These measurements suggest that more work is needed to understand potential DBP formation and human exposure within a variety of indoor environments where disinfection techniques that generate airborne microdroplets are used.

KEYWORDS: indoor chemistry, disinfection byproducts (DBPs), bleach cleaning, chlorine, halogenation, PTR-MS

## 1. INTRODUCTION

Disinfection practices targeting indoor surfaces have increased during and following the COVID-19 pandemic. 1-3 Many disinfectants utilize reactive species such as chlorine-based compounds or peroxides as the active ingredients,<sup>3</sup> which can lead to the formation of disinfection byproducts (DBPs) during indoor usage.<sup>2,4</sup> EPA-approved application methods comprise traditional techniques such as sprays or wipes, as well as more novel techniques such as electrostatic sprayers and fogging devices.<sup>3</sup> These novel devices generate microdroplets in order to disperse disinfectant-laden microdroplets to a surface or throughout an indoor space in order to achieve high surface coverage. These devices generate droplet populations with a range of different median size ranges, as shown during recent testing by the U.S. EPA.5 For many of the devices tested, ~10% of the dispersed volume was in droplets with diameter approximately 15  $\mu$ m or less and therefore may remain airborne for several minutes to hours before

deposition.<sup>6</sup> While airborne or deposited on a surface, water vapor and volatile organic compounds (VOCs) will partition either to or away from droplets to establish equilibrium within the indoor environment. Droplets will typically undergo some degree of evaporation to reach an equilibrium size based on the ambient relative humidity (RH) and droplet composition, which can prolong particle lifetime.<sup>6</sup> Volatile organic compound (VOC) emissions during indoor disinfection events arising from the partitioning of VOCs away from disinfectant solutions have been documented in prior work.<sup>4,7-9</sup> However, the partitioning of VOCs to disinfectant-covered surfaces or

Received: July 11, 2023
Accepted: September 11, 2023
Published: November 29, 2023





microdroplets may also occur during disinfectant usage due to the high surface area present in indoor environments and additional surface area created by droplet generation. <sup>7,10,11</sup>

DBP formation has been documented in a variety of settings including indoor environments and wastewater treatment. Chlorophenolic DBPs, the focus of this work, have been of concern for conferring an unpleasant taste to drinking water and producing harmful chlorocarbons 13,14 and quinones 15-17 during multigeneration reactions. These scenarios typically involve DBP formation in bulk aqueous environments, and less is known about the potential for DBP formation within microdroplets generated during spraying or fogging disinfection events. A variety of chemical reactions have been observed to greatly accelerate within microdroplets compared to bulk solution environments, <sup>18,19</sup> suggesting that chemistry occurring within or at the surface of microdroplets may be a significant or unique source of disinfection byproducts during microdropletgenerating disinfection methods. Microdroplet environments may lead to the formation of novel byproducts due to differences in solvation environment or pH compared to bulk solution. Such reactions may occur between dissolved species already present in the disinfection solution or with ambient VOCs that can partition into microdroplets or collide with droplet surfaces. In this work, we discuss the aqueous reaction between reactive chlorine species and phenol. 12,21-24 We perform a series of experiments applying commercial bleach solutions within an environmental chamber using a commercial ultrasonic humidifier to inject and disperse bleach through microdroplets and analyze the emissions with a highresolution Vocus proton transfer reaction mass spectrometer.

## 2. METHODS

Environmental chamber experiments are described in more detail in separate publications<sup>25–27</sup> and are described only briefly here. Experiments were conducted in a 67 m $^3$  (5.5 m $\times$ 4.5 m  $\times$  2.7 m) stainless steel chamber operating at  $\sim$ 23 °C with an  $\sim 2.3 \text{ h}^{-1}$  air change rate. For each experiment, 1 L of ~0.10% NaOCl bleach solution (Clorox; diluted with tap water and according to manufacturer instructions) was placed in a commercial ultrasonic misting device (Holmes HM827TG-FCA) on a laminate table and turned on to inject bleach solution as microdroplets at a rate of approximately 0.25 L hr<sup>-1</sup> until the reservoir was low (approximately 4 h). Injection using a commercial misting device is intended to distribute a large volume of bleach solution droplets throughout the chamber during the measurement period. This method would also be similar to injections achieved through commercial disinfectant electrostatic spraying or fogging devices, with the size distribution likely skewed smaller than what is typically generated while using the commercial devices. 5,28-31 The electrostatic precipitator and fogging devices evaluated by Wood et al. (2021) observed most droplets to have a diameters of tens of  $\mu m$  with ~5% of the volume in droplets with  $d < 10 \mu \text{m}$ , while commercial humidifiers can generate variable droplet size distributions that are likely in the range of hundreds of nm to several tens of  $\mu$ m.  $^{28-31}$ 

VOC measurements were performed with a Vocus 2R proton transfer reaction time-of-flight mass spectrometer (Vocus, Tofwerk AG/Aerodyne Research, Inc.). The Vocus was operated with an ion molecular reactor pressure of 2.3 mbar, 15 sccm flow rate from the water reservoir ( $H_3O^+$  source), and IMR front and back voltages of 650 and 25 V,

respectively. The E/N ratio was calculated to be 150 Td. The Vocus drew sample flow at 2.5 Lpm through an approximately 2 m PTFE tube (1/8" ID, 1/4" OD) and overflowed much of this while sub-sampling from this flow at a rate of 0.1 Lpm. Data were acquired at a rate of 1 Hz, averaged over 10 second intervals, and analyzed in Igor Pro (version 8.0.4.2, Wavemetrics) using the TofWare data analysis package (version 3.2.2.1, Tofwerk AG/Aerodyne Research, Inc.). Explicit calibrations were performed with a stepwise increasing flow from a mixed calibration gas cylinder (Apel Riemer Environmental) that was diluted with clean air from the internal generator on the Vocus. Calibrations were used to construct a correlation plot between calibrant sensitivities (cps/ppbv) and proton-transfer reaction rate coefficients  $(k_{PTR})$ , which was used to estimate measured analyte concentrations for species that were not included in the calibration gas cylinder. Analyte  $k_{\rm PTR}$  values were estimated based on previous measurements<sup>33</sup> or previously described methods based on analyte molecular formula, polarizability, and dipole moment when measurements are unavailable. <sup>33,34</sup> Parameters utilized for different analytes are given in Table S1. These methods generally yield sensitivities that agreed within 20 to 50% during prior work (with a small number of exceptions).<sup>34</sup> The uncertainty in concentration measurements of analytes without an explicit calibration is expected to be in the range of 30 to 50%.

A thermal manakin breathing system "wearing" a KN95 mask (BYD Electronics, Cueva) was used to evaluate personal VOC exposure during disinfection. Experiments were done with a dry or pre-humidified mask, with other experimental conditions identical, to approximate wearing either a fresh or well-worn mask. The pre-humidified mask was prepared before the experiment by "exhaling" humid air through the manakin onto the mask, leading to approximately 1 g of water uptake to the mask.<sup>26</sup> Mask humidification also led to an increase in chamber RH (measured with a LI-COR LI-850 H<sub>2</sub>O/CO<sub>2</sub> analyzer) to approximately 45% RH, compared to the ∼20% in the dry mask experiment that was typical of these chamber experiments.<sup>26</sup> The Vocus sampled from four separate locations during each chamber experiment with the sample location controlled by a valve switching system (Valco Instruments Co., Inc.) at a flow rate of 2.5 L/min (Lpm), while lines from the location not being actively sampled pulled at 1 Lpm. The four sampling locations were the chamber inflow, the chamber outflow, a location within the chamber approximately 20 cm in front of the manakin, and subsampling the manakin breathing line located approximately 15 cm behind the manakin mask; the chamber near-mask and behindmask positions are discussed in greater detail in this work. Chamber outflow measurements are similar to those at the near-mask position, and chamber inflow concentrations remained steady throughout the experiment. Measurements at non-inflow locations lasted 5 min each while chamber inflow was sampled for a total of 15 min for a cycle time of 30 min. Measurements at each location are reported as an average taken without the first minute of sampling to allow VOC concentrations to stabilize.

# 3. RESULTS AND DISCUSSION

**3.1. DBP Identification and Formation.** Bleach application generated a variety of primary and secondary VOCs during chamber experiments that are described in more detail in a separate publication. We here focus on the gasphase observations of the chlorophenolic DBPs shown in

Figure 1. Chlorination of the phenol reaction series. Reaction proceeds through an electrophilic aromatic substitution mechanism, where phenol (or phenolate anion) reacts with a reactive chlorine species such as HOCl (or  $OCl^-$ ,  $NH_2Cl$ , and potentially other species). The maximum rate for each chlorination step has been observed to occur at a pH slightly below the  $pK_a$  for each species. Initial chlorination adds Cl at the ortho or para positions to produce monochlorophenol (MCP), dichlorophenol (DCP), and eventually trichlorophenol (TCP). Further chlorination results in loss of aromaticity and the formation of products including 2,6-dichlorobenzoquinone (DCBQ) and 2,4,4,6-tetrachloro-2,5-cyclohexadienone (TCCHD).  $^{12,16,22,23,39-41}$  Acero et al. (2005) reported a preference for substitution at the ortho position with the products 2-chlorophenol and 4-chlorophenol formed in a 4:1 ratio and 2,6-dichlorophenol and 2,4-dichlorophenol formed in a 2.8:1 ratio.

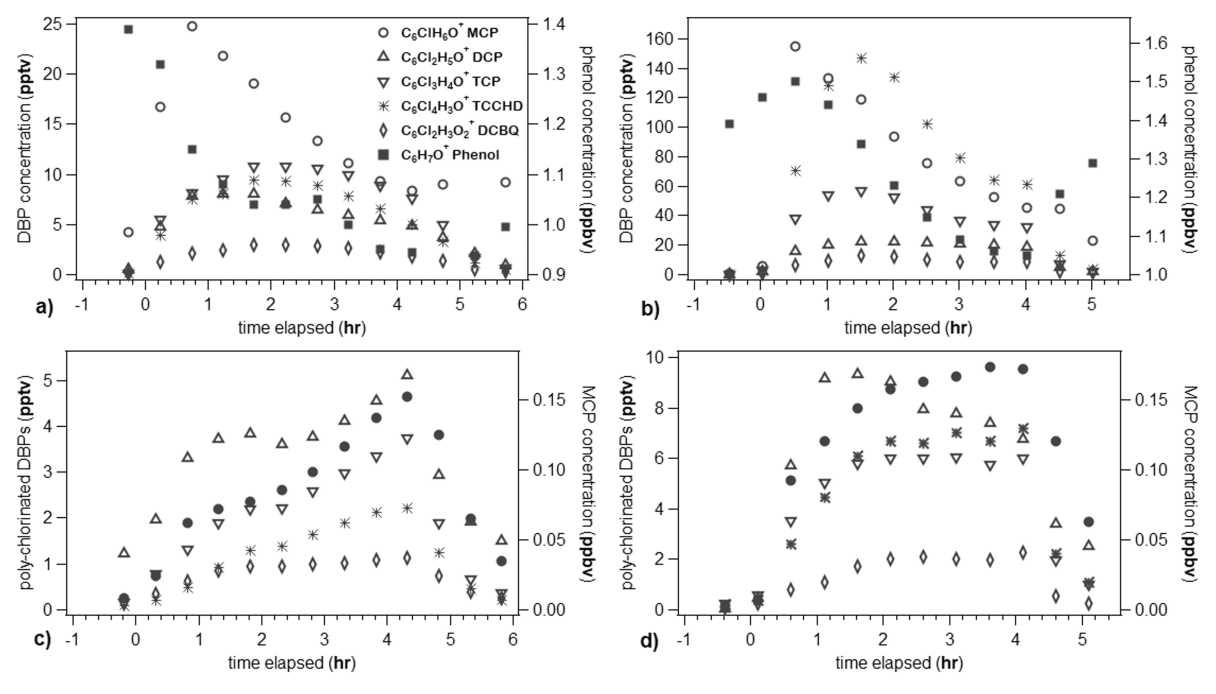


Figure 2. Chlorophenol concentration time series during bleach cleaning. Figure 2a (chamber) and c (behind-mask) show analyte concentrations during the humidified-mask experiment, while Figure 2b (chamber) and d (behind-mask) show the same for a dry-mask experiment. Symbol shapes are consistent between panels and filled symbols correspond to the right axis (note that the right axis corresponds to phenol in a and b and MCP in c and d). The time-elapsed zero-point corresponds to the beginning of injection. Note the difference in *y*-axis units and scales between left and right *y*-axes in each panel. Bleach injection lasted approximately 4 to 4.5 h based on the observed injection rate, but the exact time at which the injection reservoir was depleted could not be determined. As stated in Methods, measurement uncertainty is expected to be in the range of 30 to 50%.

Figure 1. Chlorophenolic DBPs have not been described in previous works examining gaseous emissions from bleach cleaning activities, 4,7,8,36-38 though phenol has been observed to partition to aqueous disinfectant solutions applied indoors. Previous studies on heterogeneous bleach chemistry observed a variety of volatile DBPs including chlorocarbons, chloroacids, chlorinated organic amines, and chlorinated terpenoids but did not report chlorophenols or similar DBPs. 4,7,8,36-38 Chlorophenolic DBPs have generally been studied in the context of wastewater treatment and form primarily through aqueous chlorine addition to the aromatic

ring to produce 2,4,6-trichlorophenol (TCP) as the final phenolic product,  $^{12,22,23,39-41}$  after which further chlorination forms a variety of nonaromatic products, including 2,6-dichlorobenzoquinone (DCBQ), 2,4,4,6-tetrachloro-2,5-cyclohexadienone (TCCHD), and small chlorocarbons.  $^{12,16,22,23,39-41}$  Chlorination of TCP has also been reported to form 2,3,4,6-tetrachlorophenol,  $^{41}$  but we suspect TCCHD is the primary tetrachloro species we observe. The dichloro (DCP) and trichlorophenol (TCP) molecules are detected as a protonated  $[M+H]^+$  as well as an  $[M]^+$  ion due to charge transfer (Figure S1), which is relatively efficient for

aromatic molecules. However, the  $[M]^+$  analogue of the tetrachloro molecule is present to a substantially lesser extent, suggesting that it is not aromatic. In environmental smog chamber experiments phenol chlorination has also been observed following heterogeneous reaction of condensed phenol and  $\text{Cl}_2(g)$ ; however, this reaction was only observed to produce monochlorophenol (MCP) and therefore is unlikely to be the main reaction driving phenol chlorination in our experiments. We also discuss this reaction possibility in more detail in the SI, Section S2.

The chlorophenol concentration time series during bleach usage are shown in Figure 2. A typical near-mask experimental time series is shown in Figure 2a for the dry-mask experiment. Phenol concentration decreases when application begins, indicating partitioning to bleach solution as observed in prior work, 10 and is accompanied by simultaneous growth of the chlorophenolic DBP signals. Background phenol concentrations were generally stable within the chamber ( $\sim$ 1.4 ppbv) and result from the inflow air (~1.2 ppbv) and emissions from the objects placed within the room, including the wooden table and chairs 44 and the thermal manakin. Phenol is generally considered volatile but is also relatively water-soluble with a Henry's law solubility constant of approximately 20 mol m<sup>-3</sup> Pa<sup>-1</sup>, 45 so some partitioning to aqueous media is expected. 10 The partitioning of the polychlorophenols above aqueous bleach is also governed by the Henry's law solubility constant  $K_{\rm H}$ ; while these molecules are practically nonvolatile, they are also not highly soluble, with  $K_{\rm H}$  values <sup>4S</sup> in the range of approximately 1-5 mol m<sup>-3</sup> Pa<sup>-1</sup> and are expected to partition to a measurable extent to the gas phase (see also Table S2). After bleach application concludes, chlorophenol signals steadily decrease due to deposition and air change while phenol concentrations rise.

Larger amounts of chlorophenolic DBPs are formed during the wet-mask experiment (Figure 2b,d) than during the drymask experiment. We suspect this occurs because a larger amount of phenol is present in the injected droplets, which initially causes the gas-phase phenol concentration to rise during injection (Figure 2b). This may be due to phenol leaching from the plastic of the humidifier, as phenolic species are common additives and base materials of plastics. 44,46,47 This experiment utilized a new device where the device reservoir was rinsed before usage, but the internal plumbing was not. Another difference between the dry and humidified mask experiments that may lead to differences in gas-phase observations is the chamber RH, ~20% vs 45% for the dry and humidified mask experiments, respectively. This will lead to differences in the amount of adsorbed water on chamber surfaces, which, in turn, may lead to differences in partitioning and surface adsorption of DBPs. Most of the surface area in the chamber is stainless steel and we expect these RH differences to have a small effect on the amount of adsorbed water, based on prior work that observed water surface layer growth from approximately 30 to 40 nm between these two RH values.<sup>48</sup> Chamber RH will also affect how quickly airborne droplets evaporate. Based on the RH values and the assumed particle size (hundreds of nm to low tens of  $\mu$ m),  $^{28-31}$  we expect droplet evaporation rates be similar between experiments and not impact DBP generation.<sup>6</sup> We therefore do not expect the RH differences between experiments to substantially contribute to the observed differences in gas-phase observations.

After the leached phenol is depleted, chamber phenol concentrations decrease as in the other experiment. MCP

concentration reaches a clear maximum approximately 30 min after injection begins followed by clear maxima for TCP and TCCHD near the 1.5 h mark, consistent with the reactive formation of the latter two species (Figure 1). DCP concentration remains much lower than other analytes and does not reach a clear maximum. This may be due to the larger forward reaction rate for DCP ( $\sim 1-2$  orders of magnitude higher than TCP, Figure S2) leading to greater accumulation of TCP. These rates were previously investigated in the context of wastewater treatment and may differ relative to bleach cleaning, where a larger concentration of reactive chlorine is expected; rates have been observed to be first order relative to both reactive chlorine and phenol. 12,23,40 DCP and TCP also have similar Henry's law solubilities, 45 but partitioning between the gas and aqueous phases will also be influenced by droplet pH due to differing p $K_a$  values (Figure 2). Bleach pH is likely in the range of 9.5 to 12,<sup>7–9</sup> but droplet pH is not easily estimated in the present work, in part because CO2 dissolution and water evaporation may alter droplet pH. We also observe several other ions that may also originate from phenol chlorination, based on the molecular formula and differences in ion intensity between Figure 2a and c experiments (see SI, Figure S3). Small concentrations (~1 ppt) of brominated DBPS are also observed (Figure S4): NH<sub>3</sub>Br<sup>+</sup>, bromamine; C<sub>6</sub>BrH<sub>6</sub>O<sup>+</sup>, likely monobromophenol; and C<sub>6</sub>BrCl<sub>3</sub>H<sub>2</sub>O<sup>+</sup>, likely a brominated analogue of TCCHD. Reactive bromine species may be more common in some environments<sup>22,49</sup> and brominated phenolics can have altered reaction rates, product distributions, and toxicity relative to purely chlorinated species, 22,41,49 so the observation of bromophenolic DBPs during bleach usage is notable and novel.

Several differences are observed between the chamber and behind-mask analyte time series during both dry and humidified mask experiments. During both conditions, the most apparent difference is a lower concentration of the polyhalogenated DBPs TCP and TCCHD behind the mask. In the dry-mask experiment (Figure 2d), the mask represents a potential adsorption or condensation sink for airborne compounds, and we suspect TCP and TCCHD deposit to the mask and then only volatilize to a small extent. MCP is the most volatile DBP formed and therefore is expected to be the most prevalent behind the mask, which is the case. Similarly, DCP is more volatile than TCP and TCCHD and, despite having lower abundance within the chamber, has a higher behind-mask concentration than the other DBPs (besides MCP). In contrast to a dry mask, a wet mask (Figure 2b) represents both an aqueous reaction volume and a potential condensation sink. The mask takes up approximately 1 g of H<sub>2</sub>O during humidification, creating a volume where aqueous reactions can occur. We suspect this reaction volume leads to a more rapid rise in behind-mask MCP during this experiment. Multigeneration DBPs may also form within the wet mask but may volatilize differently compared to airborne droplets due to potential adsorption to the mask material. We suspect this is why only MCP substantially increases at the behind-mask position, while DCP and the other multigeneration DBPs exhibit similar relative behavior as the dry mask experiment.

There are several aspects of our results that appear to be in contrast with prior aqueous disinfection work. Although approximately an hour passes between the concentration maxima for MCP and TCP, TCP and TCCHD reach their respective maxima at nearly identical times. This is in contrast to what would be expected based on prior work where TCP

chlorination has been observed to be the slowest step in phenol chlorination by a substantial margin, particularly at the alkaline pH values expected of bleach solution (Figure S2). 12,13 However, we note that a detailed investigation of the reaction kinetics is outside the scope of the present work. Experimental unknowns (droplet size distribution, initial bleach pH, and changes to bleach pH over time) combine to make accurate estimation of initial [HOCl]<sub>aq</sub> and [phenol]<sub>aq</sub> and molar formation rates of MCP, DCP, and TCP difficult; these considerations are discussed further in the Supporting Information, Section S3. Additionally, a known hydrolysis product of DCBQ, 3-hydroxy, 2,6-dichlorobenzoquinone (Figure S5), is not clearly detected during these experiments. DCBQ will undergo base-catalyzed hydrolysis to the hydroxy DCBQ with a half-life of 7-8 h at pH 7 and rapidly enough at pH 8 to not be detected during LC-MS analysis. 15,17 DCBQ and hydroxy DCBQ are estimated to have nearly identical Henry's law solubility constants (Table S2),<sup>50</sup> suggesting that if any appreciable amounts of hydroxy DCBQ were formed, it would partition similar to the gas phase and be detected at some time during the experiments. Lastly, we note that prior works observing TCCHD have only done so under neutral or acidic conditions (pH 3.5, 6, or 7). 14,39,51 This may indicate TCCHD is not formed under alkaline conditions or is rapidly lost to hydrolysis or other reactions, as are many halogenated DBPs. 52,53 The reasons for these differences with past observations are not immediately clear, but may relate to the unique reaction environment in our work: airborne microdroplets, as opposed to aqueous solutions. CO<sub>2</sub> will partition to airborne droplets and lower the pH through dissociation to carbonic acid, as with bulk solution; however, this would be expected to occur more rapidly within droplets due to a larger surface area to volume ratio. Microdroplets have also been observed to exhibit pH gradients with pH decreasing towards the edge of the droplet,<sup>54</sup> potentially providing a lower pH environment. A variety of reactions have also been observed to accelerate to some extent within microdroplets, which may affect the relative reaction rates for different chlorination steps. 18,19,55 Overall, unique aspects of reactions occurring within microdroplets provide plausible explanations for our

**3.2. Exposure Implications.** Our results raise potential personal exposure considerations during bleach disinfection that are relevant to both traditional bleach cleaning and airborne delivery systems. Based on prior work examining indoor partitioning and disinfection, phenol would be expected to rapidly partition to bleach solution on surfaces or in droplets<sup>10</sup> where it would then be expected to react and form DBPs; this is directly observed during the present work (Figure 2). A wide variety of chlorophenolic DBPs with welldocumented negative health impacts<sup>56</sup> can be produced, including chloroform, benzoquinones, dialdehydes, 22 small oxygenated and nitrogenated halocarbons, 14 and a variety of other structures. 52,53 Several of these DBPs are observed in the present work (Figures 2, S3, and S4) as well as some apparent DBPs whose structures are uncertain (Figure S3). Of the DBPs noted in Figure 2, DCBQ (and more broadly other halobenzoquinones, HBQs) have the strongest potential for adverse health effects. From the substantially more cytotoxic (toxic to cells) than more commonly discussed bleach DBPs, like halomethanes<sup>7,57</sup> and haloacids,<sup>38</sup> and are tentatively linked to increased bladder cancer risk from drinking chlorine-treated water. 15,56 The negative health effects

of chlorophenolic DBPs (including halocarbons, haloacids, and benzoquinones) have generally been based on an aqueous (typically ingestion) rather than inhalation exposure pathway, <sup>56</sup> and as such inhalation risk assessment would benefit from additional toxicity evaluation. The route of exposure to a toxin will influence the exposed organs and how the toxin is metabolized. For example, prior work observed trihalomethanes to be dispersed throughout more of the body when they are inhaled rather than ingested through water. <sup>58</sup> It therefore seems reasonable to expect HBQs and other DBPs to become more dispersed within the body when inhaled (either directly or through inhaled droplets) rather than ingested. It also seems reasonable to expect HBQs to have substantial adverse health effects regardless of the exposure route.

Inhalation exposure can likely be lessened by ensuring a disinfection space is well-ventilated and wearing personal protective equipment such as a mask with a charcoal adsorbent. The behind-mask concentration profiles (Figure 2c,d) and our prior work<sup>26</sup> suggest that K/N95 masks may serve as adsorbent sites, thereby lessening initial exposure. However, primary compounds and DBPs were observed to accumulate in the mask over time during disinfectant injection, and the mask eventually acted as a source for these species for several hours after disinfection application finished, as discussed in more detail in the work of Bhattacharyya et al. (2023).<sup>26</sup> DBPs that do not effectively volatilize and favorably partition to and reside on surfaces can be incorporated into indoor dust<sup>59</sup> or removed through surface contact (such as human touch or wiping) and may remain a potential exposure concern well after a disinfection event.

Structurally diverse DBPs may be expected to volatilize or remain in the condensed phase depending on individual properties and the indoor space, as discussed in prior work. 10 Volatilization from droplets rather than surfaces (as in traditional bleach cleaning) represents a process with different partitioning considerations. Droplets will likely have a higher surface-area-to-volume ratio than an aqueous surface layer that will enable DBP volatilization to occur more rapidly, 60 leading to a faster expected rise in air concentrations while also potentially interrupting further condensed-phase reaction and loss. Additionally, an airborne bleach droplet is, presumably, an aqueous salt droplet without a substantial organic phase that lacks other potential adsorption or absorption sites, which would limit the ability of a DBP to partition away from the aqueous phase while remaining in the condensed phase. We do note that NaOCl-based disinfectants are typically not pure NaOCl and added organics and other salts may influence particle phase and morphology while airborne, particularly after some degree of evaporation has occurred. An organic layer is commonly found on indoor surfaces, 61,62 and many of the DBPs we discuss here have  $K_{OW} > 1$  (Table S2<sup>50</sup>), indicating a preference for the organic layer. Chlorinated species can effectively adsorb to common indoor materials,<sup>63</sup> which would also limit DBP volatilization from surfaces. These factors combine to make chlorinated DBP volatilization from airborne droplets more feasible than from surfaces, which likely contributes to our gas-phase observations of chlorophenolic DBPs that may not have been observed in prior measurements. 4,7,8,36–38

A basic aspect of DBP formation is that formed DBPs depend on potential reactants within the disinfection space. Indoor concentrations of phenol will vary depending on potential source materials such as volatile chemical products

(VCPs), wood, and plastics. 8,13,14,44 A chamber phenol concentration of ~1.4 ppbv was observed in the present work (Figure 2), while past measurements of a residence<sup>44</sup> and the UT Test House model residence<sup>8</sup> observed average phenol concentrations of ~0.5 and 0.4 ppbv, respectively. Residential measurements also observed ratios >1 between indoor and outdoor phenol concentrations, 8,44 indicating indoor materials or activities were the primary source. Outdoor air masses influenced by biomass burning emissions may also contain substantial amounts of phenol, 64,65 leading to a potential outdoor-to-indoor source in some scenarios. More highly substituted hydroxybenzenes, with similar  $K_{\rm H}$  values, <sup>45</sup> such as catechol or cresol, would also be expected to behave similarly to phenol during disinfection and partition to bleach solution to undergo chlorination reactions. 13,14,16,22 Indoor concentrations of more functionalized phenolic species would likely be lower than phenol in most scenarios but will again vary with indoor materials 14,44,47 and be influenced by biomass burning emissions.<sup>64,65</sup> Different phenolic compounds have different branching ratios during DBP formation, <sup>13,14,16,22</sup> potentially leading to more diverse or toxic DBP formation in some scenarios. Spaces influenced by biomass burning emissions, in particular, would likely be prone to a high degree of chlorophenolic DBP formation during bleach cleaning. The presence of other halide anions can also influence DBP products and accelerate formation rates to produce DBPs with a higher level of toxicity. <sup>22,24,41,49</sup> This has been observed with both bromide and iodide, both of which may be present in water used to dilute bleach prior to cleaning. 22,24,41,49 The differing toxicity of polyhalogenated compared to polychlorinated DBPs and relatively faster addition to phenolic species means that small amounts of bromide or iodide would likely be able to exert a relatively large influence on harmful DBP formation. For the brominated DBPs we observed, it is not clear whether the incorporated bromine was present in the initial bleach or originated from the added tap water.

#### 4. SIGNIFICANCE AND IMPLICATIONS

We describe the formation of a series of primarily chlorophenolic and bromophenolic DBPs during the injection of bleach microdroplets into an environmental chamber. The observation of these DBPs is notable as they have not been reported in prior bleach work<sup>4,7,8</sup> and for their potential adverse health impacts, particularly the toxic benzoquinone DCBQ. 13-16 The product distribution and formation rates appear to reflect a lower pH environment and altered reaction kinetics relative to those of highly alkaline bulk bleach, which we attribute to the unique reaction environment of airborne microdroplets. A chamber phenol concentration of approximately 1.0-1.5 ppbv was observed during the measurement campaign, and the availability of phenol appeared to limit the extent of reaction. More highly chlorinated, less volatile DBPs are observed to deposit to and not substantially volatilize from both wet and dry KN95 masks used for evaluating personal exposure, indicating that these DBPs volatilized more effectively from the airborne microdroplets than this surface. This observation and estimated partitioning constants (Table S2) suggest that these DBPs will ultimately reside primarily on indoor surfaces after they form (though different materials will have different adsorption characteristics<sup>63</sup>) and, if they form on a surface during traditional bleach cleaning or after droplet deposition, may not volatilize to sufficient degree to be detected. Airborne microdroplets generated while using

modern disinfection application techniques, including fogging and electrostatic spraying devices,<sup>5</sup> represent potentially unique DBP exposure pathways due to the unique reaction and volatilization environments of airborne microdroplets. DBP exposure resulting from droplet generation techniques will include direct inhalation of volatilized DBPs as well as exposure to microdroplets through inhalation or dermal contact. Although we primarily discuss chlorophenolic DBPs, in realistic usage scenarios, they will be one component of a much larger range of DBPs that combine to yield the complete potential for adverse health effects from short- or long-term exposure. This work demonstrates that disinfection techniques utilizing droplet generation do indeed represent unique DBP formation and dispersal pathways relative to traditional techniques and that these techniques merit further study to better understand DBP formation and personal exposure within the variety of potential indoor environments where disinfection may be performed.<sup>2</sup>

## ASSOCIATED CONTENT

## Supporting Information

The Supporting Information is available free of charge at https://pubs.acs.org/doi/10.1021/acsestair.3c00011.

Information on peak identification and quantification, prior literature on aqueous phenol chlorination rates, additional DBP time series, and DBP partitioning values (PDF)

## AUTHOR INFORMATION

## **Corresponding Author**

Leif G. Jahn — McKetta Department of Chemical Engineering, University of Texas at Austin, Austin, Texas 78712, United States; orcid.org/0000-0002-5616-4448; Email: leif.jahn@austin.utexas.edu

## **Authors**

Nirvan Bhattacharyya – McKetta Department of Chemical Engineering, University of Texas at Austin, Austin, Texas 78712, United States; orcid.org/0000-0003-3911-6492

Daniel Blomdahl — Department of Civil, Architectural, and Environmental Engineering, University of Texas at Austin, Austin, Texas 78712, United States; ○ orcid.org/0000-0002-2004-0937

Mengjia Tang — Department of Civil, Architectural, and Environmental Engineering, University of Texas at Austin, Austin, Texas 78712, United States; Present Address: Oak Ridge National Lab, 1 Bethel Valley Rd., Oak Ridge, TN 37830, U.S.A; © orcid.org/0000-0002-6721-5626

Pearl Abue – McKetta Department of Chemical Engineering, University of Texas at Austin, Austin, Texas 78712, United States

Atila Novoselac — Department of Civil, Architectural, and Environmental Engineering, University of Texas at Austin, Austin, Texas 78712, United States

Lea Hildebrandt Ruiz — McKetta Department of Chemical Engineering, University of Texas at Austin, Austin, Texas 78712, United States; orcid.org/0000-0001-8378-1882

Pawel K. Misztal – Department of Civil, Architectural, and Environmental Engineering, University of Texas at Austin, Austin, Texas 78712, United States; ○ orcid.org/0000-0003-1060-1750

Complete contact information is available at:

## https://pubs.acs.org/10.1021/acsestair.3c00011

## **Author Contributions**

L.G.J. conducted the analysis and wrote the manuscript. All authors contributed to the set up and performance of experiments, as well as to the review and revision of the manuscript.

#### **Notes**

The authors declare no competing financial interest.

## ACKNOWLEDGMENTS

This material is based on work supported by the National Science Foundation under Grant Nos. 2027420 and 2146347. This material is based in part on work supported by the Alfred P. Sloan Foundation under Grant No. G-2018-11240 and the National Science Foundation Grant No. 2146347. L.G.J. was supported by the Camille and Henry Postdoctoral Program in Environmental Chemistry. We thank all sponsors for their generous support.

## REFERENCES

- (1) Hora, P. I.; Pati, S. G.; McNamara, P. J.; Arnold, W. A. Increased Use of Quaternary Ammonium Compounds during the SARS-CoV-2 Pandemic and Beyond: Consideration of Environmental Implications. *Environ. Sci. Technol. Lett.* **2020**, *7* (9), 622–631.
- (2) Collins, D. B.; Farmer, D. K. Unintended Consequences of Air Cleaning Chemistry. *Environ. Sci. Technol.* **2021**, *55* (18), 12172–12179.
- (3) United States Environmental Protection Agency. EPA List N Disinfectant Results Table; EPA, 2020, No. 1, pp 1–57.
- (4) Farmer, D. K.; Vance, M. E.; Abbatt, J. P. D.; Abeleira, A.; Alves, M. R.; Arata, C.; Boedicker, E.; Bourne, S.; Cardoso-Saldaña, F.; Corsi, R.; Decarlo, P. F.; Goldstein, A. H.; Grassian, V. H.; Hildebrandt Ruiz, L.; Jimenez, J. L.; Kahan, T. F.; Katz, E. F.; Mattila, J. M.; Nazaroff, W. W.; Novoselac, A.; O'Brien, R. E.; Or, V. W.; Patel, S.; Sankhyan, S.; Stevens, P. S.; Tian, Y.; Wade, M.; Wang, C.; Zhou, S.; Zhou, Y. Overview of HOMEChem: House Observations of Microbial and Environmental Chemistry. *Environ. Sci. Process Impacts* 2019, 21 (8), 1280–1300.
- (5) Wood, J. P.; Magnuson, M.; Touati, A.; Gilberry, J.; Sawyer, J.; Chamberlain, T.; McDonald, S.; Hook, D. Evaluation of Electrostatic Sprayers and Foggers for the Application of Disinfectants in the Era of SARS-CoV-2. *PLoS One* **2021**, *16* (9), No. e0257434.
- (6) Morawska, L. Droplet Fate in Indoor Environments, or Can We Prevent the Spread of Infection? *Indoor Air* **2006**, *16*, 335–347.
- (7) Mattila, J. M.; Lakey, P. S. J.; Shiraiwa, M.; Wang, C.; Abbatt, J. P. D.; Arata, C.; Goldstein, A. H.; Ampollini, L.; Katz, E. F.; DeCarlo, P. F.; Zhou, S.; Kahan, T. F.; Cardoso-Saldaña, F. J.; Ruiz, L. H.; Abeleira, A.; Boedicker, E. K.; Vance, M. E.; Farmer, D. K. Multiphase Chemistry Controls Inorganic Chlorinated and Nitrogenated Compounds in Indoor Air during Bleach Cleaning. *Environ. Sci. Technol.* 2020, 54 (3), 1730–1739.
- (8) Arata, C.; Misztal, P. K.; Tian, Y.; Lunderberg, D. M.; Kristensen, K.; Novoselac, A.; Vance, M. E.; Farmer, D. K.; Nazaroff, W. W.; Goldstein, A. H. Volatile Organic Compound Emissions during HOMEChem. *Indoor Air* **2021**, *31* (6), 2099–2117.
- (9) Wong, J. P. S.; Carslaw, N.; Zhao, R.; Zhou, S.; Abbatt, J. P. D. Observations and Impacts of Bleach Washing on Indoor Chlorine Chemistry. *Indoor Air* **2017**, 27 (6), 1082–1090.
- (10) Wang, C.; Collins, D. B.; Arata, C.; Goldstein, A. H.; Mattila, J. M.; Farmer, D. K.; Ampollini, L.; DeCarlo, P. F.; Novoselac, A.; Vance, M. E.; Nazaroff, W. W.; Abbatt, J. P. D. Surface Reservoirs Dominate Dynamic Gas-Surface Partitioning of Many Indoor Air Constituents. *Sci. Adv.* **2020**, *6* (8), No. eaay8973.
- (11) Lunderberg, D. M.; Kristensen, K.; Tian, Y.; Arata, C.; Misztal, P. K.; Liu, Y.; Kreisberg, N.; Katz, E. F.; DeCarlo, P. F.; Patel, S.; Vance, M. E.; Nazaroff, W. W.; Goldstein, A. H. Surface Emissions

- Modulate Indoor SVOC Concentrations through Volatility-Dependent Partitioning, *Environ. Sci. Technol.* **2020**, *54* (11), *6751–6760*.
- (12) Lee, G. F.; Morris, J. C. Kinetics of Chlorination of Phenolchlorophenolic Tastes and Odors. *Int. J. Air Water Pollution* **1962**, *6*, 419–431.
- (13) Gallard, H.; von Gunten, U. Chlorination of Phenols: Kinetics and Formation of Chloroform. *Environ. Sci. Technol.* **2002**, *36* (5), 884–890.
- (14) Chuang, Y. H.; McCurry, D. L.; Tung, H. H.; Mitch, W. A. Formation Pathways and Trade-Offs between Haloacetamides and Haloacetaldehydes during Combined Chlorination and Chloramination of Lignin Phenols and Natural Waters. *Environ. Sci. Technol.* **2015**, *49* (24), 14432–14440.
- (15) Qin, F.; Zhao, Y.-Y.; Zhao, Y.; Boyd, J. M.; Zhou, W.; Li, X.-F. A Toxic Disinfection By-Product, 2,6-Dichloro-1,4-Benzoquinone, Identified in Drinking Water. *Angew. Chem., Int. Ed.* **2010**, 49 (4), 790–792.
- (16) Kosaka, K.; Nakai, T.; Hishida, Y.; Asami, M.; Ohkubo, K.; Akiba, M. Formation of 2,6-Dichloro-1,4-Benzoquinone from Aromatic Compounds after Chlorination. *Water Res.* **2017**, *110*, 48–55.
- (17) Zhao, Y.; Anichina, J.; Lu, X.; Bull, R. J.; Krasner, S. W.; Hrudey, S. E.; Li, X.-F. Occurrence and Formation of Chloro- and Bromo-Benzoquinones during Drinking Water Disinfection. *Water Res.* **2012**, *46* (14), 4351–4360.
- (18) Jacobs, M. I.; Davis, R. D.; Rapf, R. J.; Wilson, K. R. Studying Chemistry in Micro-Compartments by Separating Droplet Generation from Ionization. *J. Am. Soc. Mass Spectrom* **2019**, *30* (2), 339–343.
- (19) Yan, X.; Bain, R. M.; Cooks, R. G. Organic Reactions in Microdroplets: Reaction Acceleration Revealed by Mass Spectrometry. *Angew. Chem., Int. Ed.* **2016**, *55* (42), 12960–12972.
- (20) Wei, H.; Vejerano, E. P.; Leng, W.; Huang, Q.; Willner, M. R.; Marr, L. C.; Vikesland, P. J. Aerosol Microdroplets Exhibit a Stable PH Gradient. *Proc. Natl. Acad. Sci. U. S. A.* **2018**, *115* (28), 7272–7277.
- (21) Deborde, M.; von Gunten, U. Reactions of Chlorine with Inorganic and Organic Compounds during Water Treatment-Kinetics and Mechanisms: A Critical Review. *Water Res.* **2008**, *42* (1-2), 13–51
- (22) Prasse, C.; von Gunten, U.; Sedlak, D. L. Chlorination of Phenols Revisited: Unexpected Formation of  $\alpha,\beta$ -Unsaturated C 4 -Dicarbonyl Ring Cleavage Products. *Environ. Sci. Technol.* **2020**, 54 (2), 826–834.
- (23) Núñez-Gaytán, A. M.; Vera-Avila, L. E.; De Llasera, M. G.; Covarrubias-Herrera, R. Speciation and Transformation Pathways of Chlorophenols Formed from Chlorination of Phenol at Trace Level Concentration. J. Environ. Sci. Health A Tox Hazard Subst Environ. Eng. 2010, 45 (10), 1217–1226.
- (24) Vikesland, P. J.; Fiss, E. M.; Wigginton, K. R.; McNeill, K.; Arnold, W. A. Halogenation of Bisphenol-A, Triclosan, and Phenols in Chlorinated Waters Containing Iodide. *Environ. Sci. Technol.* **2013**, 47 (13), 6764–6772.
- (25) Tang, M.; Blomdahl, D. C.; Bhattacharyya, N.; Jahn, L. G.; Abue, P.; Ruiz, L. H.; Misztal, P. K.; Novoselac, A. Chamber Study on the Dynamics of Water and Primary Compounds in the Gas Phase Following Disinfection. Manuscript in preparation, 2023.
- (26) Bhattacharyya, N.; Tang, M.; Blomdahl, D. C.; Jahn, L. G.; Abue, P.; Allen, D. T.; Corsi, R. L.; Novoselac, A.; Misztal, P. K.; Hildebrandt Ruiz, L. Bleach Emissions Interact Substantially with Surgical and KN95 Mask Surfaces. *Environ. Sci. Technol.* **2023**, 57 (16), 6589–6598.
- (27) Jahn, L. G.; Tang, M.; Blomdahl, D.; Bhattacharyya, N.; Abue, P.; Novoselac, A.; Ruiz, L. H.; Misztal, P. K. Volatile Organic Compound (VOC) Emissions from the Usage of Benzalkonium Chloride and Other Disinfectants Based on Quaternary Ammonium Compounds. *Environmental Science: Atmospheres* **2023**, *3* (2), 363–373.
- (28) Feng, Z.; Zhou, X.; Xu, S.; Ding, J.; Cao, S. J. Impacts of Humidification Process on Indoor Thermal Comfort and Air Quality

- Using Portable Ultrasonic Humidifier. Build Environ 2018, 133, 62-72.
- (29) Highsmith, V. R.; Hardy, R. J.; Costa, D. L.; Germani, M. S. Physical and Chemical Characterization of Indoor Aerosols Resulting from the Use of Tap Water in Portable Home Humidifiers. *Environ. Sci. Technol.* **1992**, *26* (4), 673–680.
- (30) Rodes, C.; Smith, T.; Crouse, R.; Ramachandran, G. Measurements of the Size Distribution of Aerosols Produced by Ultrasonic Humidification. *Aerosol Science and Technology* **1990**, *13* (2), 220–229.
- (31) Sain, A. E.; Zook, J.; Davy, B. M.; Marr, L. C.; Dietrich, A. M. Size and Mineral Composition of Airborne Particles Generated by an Ultrasonic Humidifier. *Indoor Air* **2018**, 28 (1), 80–88.
- (32) Krechmer, J.; Lopez-Hilfiker, F.; Koss, A.; Hutterli, M.; Stoermer, C.; Deming, B.; Kimmel, J.; Warneke, C.; Holzinger, R.; Jayne, J.; Worsnop, D.; Fuhrer, K.; Gonin, M.; de Gouw, J. Evaluation of a New Reagent-Ion Source and Focusing Ion-Molecule Reactor for Use in Proton-Transfer-Reaction Mass Spectrometry. *Anal Chem.* **2018**, *90* (20), 12011–12018.
- (33) Pagonis, D.; Sekimoto, K.; de Gouw, J. A Library of Proton-Transfer Reactions of H <sub>3</sub> O <sup>+</sup> Ions Used for Trace Gas Detection. *J. Am. Soc. Mass Spectrom* **2019**, 30 (7), 1330–1335.
- (34) Sekimoto, K.; Li, S.-M.; Yuan, B.; Koss, A.; Coggon, M.; Warneke, C.; de Gouw, J. Calculation of the Sensitivity of Proton-Transfer-Reaction Mass Spectrometry (PTR-MS) for Organic Trace Gases Using Molecular Properties. *Int. J. Mass Spectrom* **2017**, 421, 71–94.
- (35) Rim, D.; Novoselac, A. Transport of Particulate and Gaseous Pollutants in the Vicinity of a Human Body. *Build Environ* **2009**, 44 (9), 1840–1849.
- (36) Wang, C.; Collins, D. B.; Abbatt, J. P. D. Indoor Illumination of Terpenes and Bleach Emissions Leads to Particle Formation and Growth. *Environ. Sci. Technol.* **2019**, 53 (20), 11792–11800.
- (37) Moravek, A.; VandenBoer, T. C.; Finewax, Z.; Pagonis, D.; Nault, B. A.; Brown, W. L.; Day, D. A.; Handschy, A. V.; Stark, H.; Ziemann, P.; Jimenez, J. L.; de Gouw, J. A.; Young, C. J. Reactive Chlorine Emissions from Cleaning and Reactive Nitrogen Chemistry in an Indoor Athletic Facility. *Environ. Sci. Technol.* **2022**, *56* (22), 15408–15416.
- (38) Mattila, J. M.; Arata, C.; Wang, C.; Katz, E. F.; Abeleira, A.; Zhou, Y.; Zhou, S.; Goldstein, A. H.; Abbatt, J. P. D.; DeCarlo, P. F.; Farmer, D. K. Dark Chemistry during Bleach Cleaning Enhances Oxidation of Organics and Secondary Organic Aerosol Production Indoors. *Environ. Sci. Technol. Lett.* **2020**, *7* (11), 795–801.
- (39) Smith, J. G.; Lee, S. F.; Netzer, A. Chlorination in Dilute Aqueous Systems; 2,4,6-Trichlorophenol. *Environ. Lett.* **1975**, *10* (1), 47–52.
- (40) Ge, F.; Zhu, L.; Chen, H. Effects of PH on the Chlorination Process of Phenols in Drinking Water. *J. Hazard Mater.* **2006**, *133* (1-3), 99–105.
- (41) Acero, J. L.; Piriou, P.; Von Gunten, U. Kinetics and Mechanisms of Formation of Bromophenols during Drinking Water Chlorination: Assessment of Taste and Odor Development. *Water Res.* **2005**, *39* (13), 2979–2993.
- (42) Platz, J.; Nielsen, O. J.; Wallington, T. J.; Ball, J. C.; Hurley, M. D.; Straccia, A. M.; Schneider, W. F.; Sehested, J. Atmospheric Chemistry of the Phenoxy Radical, C6H5O(●): UV Spectrum and Kinetics of Its Reaction with NO, NO2, and O2. *J. Phys. Chem. A* 1998, 102 (41), 7964−7974.
- (43) Rose, M. R.; Lau, S. S.; Prasse, C.; Sivey, J. D. Exotic Electrophiles in Chlorinated and Chloraminated Water: When Conventional Kinetic Models and Reaction Pathways Fall Short. *Environ. Sci. Technol. Lett.* **2020**, *7* (6), 360–370.
- (44) Liu, Y.; Misztal, P. K.; Xiong, J.; Tian, Y.; Arata, C.; Weber, R. J.; Nazaroff, W. W.; Goldstein, A. H. Characterizing Sources and Emissions of Volatile Organic Compounds in a Northern California Residence Using Space- and Time-resolved Measurements. *Indoor Air* **2019**, *29* (4), ina.12562.

- (45) Sander, R. Compilation of Henry's Law Constants (Version 4.0) for Water as Solvent. *Atmos Chem. Phys.* **2015**, *15* (8), 4399–4981
- (46) Capolupo, M.; Sørensen, L.; Jayasena, K. D. R.; Booth, A. M.; Fabbri, E. Chemical Composition and Ecotoxicity of Plastic and Car Tire Rubber Leachates to Aquatic Organisms. *Water Res.* **2020**, *169*, 115270
- (47) Beel, G.; Langford, B.; Carslaw, N.; Shaw, D.; Cowan, N. Temperature Driven Variations in VOC Emissions from Plastic Products and Their Fate Indoors: A Chamber Experiment and Modelling Study. Science of The Total Environment 2023, 881, 163497.
- (48) A Manaf, N. D.; Fukuda, K.; Subhi, Z. A.; Mohd Radzi, M. F. Influences of Surface Roughness on the Water Adsorption on Austenitic Stainless Steel. *Tribol Int.* **2019**, *136*, 75–81.
- (49) Zhai, H.; Zhang, X. Formation and Decomposition of New and Unknown Polar Brominated Disinfection Byproducts during Chlorination. *Environ. Sci. Technol.* **2011**, *45* (6), 2194–2201.
- (50) United States Environmental Protection Agency. *Estimation Programs Interface Suite for Microsoft Windows*, v3.20; U.S. EPA: Washington DC, 2022.
- (51) Heasley, V. L.; Fisher, A. M.; Herman, E. E.; Jacobsen, F. E.; Miller, E. W.; Ramirez, A. M.; Royer, N. R.; Whisenand, J. M.; Zoetewey, D. L.; Shellhamer, D. F. Investigations of the Reactions of Monochloramine and Dichloramine with Selected Phenols: Examination of Humic Acid Models and Water Contaminants. *Environ. Sci. Technol.* **2004**, *38* (19), 5022–5029.
- (52) Yang, M.; Zhang, X.; Liang, Q.; Yang, B. Application of (LC/)MS/MS Precursor Ion Scan for Evaluating the Occurrence, Formation and Control of Polar Halogenated DBPs in Disinfected Waters: A Review. *Water Research* **2019**, *158*, 322–337.
- (53) Pan, Y.; Li, W.; Li, A.; Zhou, Q.; Shi, P.; Wang, Y. A New Group of Disinfection Byproducts in Drinking Water: Trihalo-Hydroxy-Cyclopentene-Diones. *Environ. Sci. Technol.* **2016**, *50* (14), 7344–7352.
- (54) Jing, X.; Chen, Z.; Huang, Q.; Liu, P.; Zhang, Y.-H. Spatiotemporally Resolved PH Measurement in Aerosol Microdroplets Undergoing Chloride Depletion: An Application of In Situ Raman Microspectrometry. *Anal Chem.* **2022**, *94* (43), 15132–15138.
- (55) Wei, Z.; Li, Y.; Cooks, R. G.; Yan, X. Accelerated Reaction Kinetics in Microdroplets: Overview and Recent Developments. *Annu. Rev. Phys. Chem.* **2020**, *71* (1), 31–51.
- (56) Li, J.; Wang, W.; Moe, B.; Wang, H.; Li, X. F. Chemical and Toxicological Characterization of Halobenzoquinones, an Emerging Class of Disinfection Byproducts. *Chem. Res. Toxicol.* **2015**, 28 (3), 306–318.
- (57) Odabasi, M. Halogenated Volatile Organic Compounds from the Use of Chlorine-Bleach- Containing Household Products. *Environ. Sci. Technol.* **2008**, 42 (5), 1445–1451.
- (58) Weisel, C. P.; Jo, W. K. Ingestion, Inhalation, and Dermal Exposures to Chloroform and Trichloroethene from Tap Water. *Environ. Health Perspect* **1996**, *104* (1), 48–51.
- (59) Lucattini, L.; Poma, G.; Covaci, A.; de Boer, J.; Lamoree, M. H.; Leonards, P. E. G. A Review of Semi-Volatile Organic Compounds (SVOCs) in the Indoor Environment: Occurrence in Consumer Products, Indoor Air and Dust. *Chemosphere* **2018**, *201*, 466–482.
- (60) Shiraiwa, M.; Pfrang, C.; Pöschl, U. Kinetic Multi-Layer Model of Aerosol Surface and Bulk Chemistry (KM-SUB): The Influence of Interfacial Transport and Bulk Diffusion on the Oxidation of Oleic Acid by Ozone. *Atmos Chem. Phys.* **2010**, *10* (8), 3673–3691.
- (61) Lim, C. Y.; Abbatt, J. P. Chemical Composition, Spatial Homogeneity, and Growth of Indoor Surface Films. *Environ. Sci. Technol.* **2020**, 54 (22), 14372–14379.
- (62) Weschler, C. J.; Nazaroff, W. W. Growth of Organic Films on Indoor Surfaces. *Indoor Air* **2017**, *27*, 1101–1112.
- (63) Won, D.; Corsi, R. L.; Rynes, M. Sorptive Interactions between VOCs and Indoor Materials. *Indoor Air* **2001**, *11* (4), 246–256.
- (64) Akagi, S. K.; Yokelson, R. J.; Wiedinmyer, C.; Alvarado, M. J.; Reid, J. S.; Karl, T.; Crounse, J. D.; Wennberg, P. O. Emission Factors

for Open and Domestic Biomass Burning for Use in Atmospheric Models. *Atmos Chem. Phys.* **2011**, *11* (9), 4039–4072.

(65) Yokelson, R. J.; Burling, I. R.; Gilman, J. B.; Warneke, C.; Stockwell, C. E.; de Gouw, J.; Akagi, S. K.; Urbanski, S. P.; Veres, P.; Roberts, J. M.; Kuster, W. C.; Reardon, J.; Griffith, D. W. T.; Johnson, T. J.; Hosseini, S.; Miller, J. W.; Cocker III, D. R.; Jung, H.; Weise, D. R. Coupling Field and Laboratory Measurements to Estimate the Emission Factors of Identified and Unidentified Trace Gases for Prescribed Fires. *Atmos Chem. Phys.* **2013**, *13* (1), 89–116.